

Projectile Attack of Surface Scattered Munitions Comparing Closed Form Theory with Live Trials

Robert J. Almond*

Senior Research Engineer, Energetic Technology Department, Dstl, Fort Halstead, Kent (UK)

Stephen G. Murray

Head of Explosive Ordnance Engineering, Royal Military College of Science, Shrivenham, Wiltshire (UK)

Abstract

This paper describes research that has been undertaken to develop a low-cost vehicle-mounted gun system to provide for the rapid disposal of surface deployed munitions (principally mines) from up to 100 m distance. Inert high-shock projectiles with optimized internal, external and terminal ballistic performance have been developed during this study. Work on shock wave interaction was reviewed in terms of the Rankine-Hugoniot jump equations, and Walker and Wasley criterion has been employed using two modifications from James to predict initiation in this divergent shock application.

Keywords: Impact Initiation, Critical Energy, Prompt Shock Initiation, Landmine Neutralization

1 Introduction

A study of worldwide in-service scatterable anti-tank mines indicated that Composition B (RDX 60%, TNT 40%) was the prevalent energetic filling. Further evaluation has identified typical charge size, common casing materials and probable kill mechanisms. Literature has been reviewed regarding prompt shock initiation, considering shock wave interaction in terms of the Rankine-Hugoniot jump equations. Impact detonation parameters have been predicted using James modified Walker and Wasley criterion, and run distances have been calculated using Popolato data. These combined theories have been evaluated against a program of live firing trials with a variety of casing materials. During this research high-shock Flat Front (FF) and low drag Shock Point (SP) projectile designs have been investigated. A 0.50 caliber vehicle-mounted gun system has been considered for deployment, with targeting effected by a remote operator CCTV over an intended range of 100 m.

2 Previous Research

James, Haskins and Cook explored [1] the effects of flat front and conical projectile impact against plastic explo-

sives, confirming initiation events were consistent with a shock to detonation transition (SDT). Hydro-code models representing divergent shock have also been verified, and overall results have demonstrated the flat front projectiles superior shock performance. Further work by Cook, Haskins and James [2, 3] investigated the effect of projectile diameter and various barriers, experimental results correlating to within 15% of a James modified Walker and Wasley equation. Their investigation also proved that initiation response is not influenced by projectile spin. Johansson and Persson [4] considered the effect of angular error on shock performance. Their results showed no significant difference for attack angles up to 4°, a progressive reduction until 8°, after which there is a sharp fall in shock pressure.

3 Theory Review

In order to calculate the projectile velocity required for a prompt shock initiation, knowledge of Hugoniot data in the P-u plane must first be developed. Here, impedance matching can ensure maximum shock pressure from a given impact scenario, and Table 1 shows Hugoniot derived data for some potential projectile materials on contact with the explosive Composition B [5, 6]. Beginning with the U-u plane material Hugoniot data for target and projectile [7, 8], shock pressure is first calculated by applying a momentum conservation equation across the impact interface.

Shown below, these calculations provide the P-u plane Hugoniot. The shock pressure figures shown in Table 1 have been derived subsequently by considering a relative projectile velocity of 1100 m/s.

$$U = C_0 + s \cdot u \quad (1)$$

$$P = \rho_0 \cdot u \cdot U \quad (2)$$

$$P_1 = \rho_0 \cdot C_0(u_1 - u_0) + \rho_0 \cdot s(u_1 - u_0)^2 \quad (3)$$

A successful prompt shock initiation is dependent on sufficient impact pressure and the duration for which it

* Corresponding author; e-mail: RALMOND@mail.dstl.gov.uk

Table 1. Material selection considering an 1100 m/s impact with Composition B.

Material	Shock Pressure GPa	Run to Detonation in mm	Comments
Platinum	7.72	7.67	Expensive
Tungsten	7.70	7.69	Processing
Uranium/Mo	7.29	8.27	Toxic
Copper	6.81	9.04	Compromise
Brass	6.61	9.41	Easy to Machine
Iron	6.52	9.58	Cheap

exists within the explosive material. Following from calculation of pressure, two techniques have been employed to assess a threshold for prompt shock initiation. Various forms of critical energy theory consider the effect of impact geometry on shock duration, and Pop Plots describe the distance (or time) for which shock must run inside the explosive before a full detonation develops. Considering the data in Table 1, Platinum and Tungsten have shown best shock performance. However, the more practical properties of Copper and Brass have led to their selection for this research.

3.1 Critical Energy Theory

Walker and Wasley introduced theory specific to one dimensional shock in 1969 [9]. Although these data are listed in many publications [7, 8], only order of magnitude accuracy can be expected when the theory is applied to divergent shock applications. To overcome this problem, James [10, 11] has progressed these equations through the two modified forms shown in Eq. (4) and Eq. (5), each allowing for a selection of projectile geometry.

$$E_C = P \cdot u_x \cdot D / (n \cdot c_x) \quad (4)$$

$$E_C = (u_x^2 - 2 \cdot \Sigma c_x) \rho_o \cdot U \cdot t_D \quad (5)$$

where $t_D = D/6c_x$ for a flat ended rod projectile

Having established shock pressure levels and particle velocity within the explosive, the onset of SDT has been predicted using these modified equations. Calculated im-

pact energy has been compared with a critical energy value of 1.85 MJ/m² quoted for Composition B [8].

Shown in Table 2, impact energy values have been calculated over the projectile velocity range, using both single and dual parameter modifications from James. The single parameter model indicates that the critical energy value and therefore prompt shock initiation will occur above a threshold velocity of 783 m/s.

Data required for the dual parameter equation are not yet subject to general publication. However, figures appropriate for the Composition-B used in these experiments [12] take activation energy (Σc) to be 60 kJ/kg with a critical energy value (refined for this compound model) of 1.95 MJ/m². Given this information, the dual parameter model indicates that prompt shock initiation should occur above a threshold velocity of 896 m/s, around 14% faster than that predicted by single parameter model.

3.2 Pop Plots and Run-Distance to Detonation

The Popolato [7] approach is also employed after calculation of impact shock pressure and describes a logarithmic relationship between shock pressure and the detonation run distance. The characteristics for Composition-B at a density of 1720 kg/m³ are given by Eq. (6).

$$\text{Log } P = 1.5587 - 0.7614 \text{ Log } x^* \quad (6)$$

Composition B at a density of 1720 kg/m³

Popolato's formula has been used to plot this relationship in Figure 1, where Composition-B is shown in comparison with two other explosives. Corresponding run distance values have been calculated against our projectile velocity break points, and these values are shown in association with the critical energy data of Table 2. In practice, initiation will only occur if the required pressure can be maintained over that distance, and pressure levels are always eroded by a release wave emanating from the projectiles periphery. A historical rule of thumb useful with rod projectiles estimates the maximum credible distance to be root two times the projectile diameter. In this application, an expected run distance of 17.75 mm indicates a threshold velocity close to 766 m/s, placing this approximate reckoning in close agreement with the single parameter critical energy criterion.

Table 2. Brass impacting Composition B, shock energy and run distance.

Projectile Velocity m/s	Shock Velocity in Explosive m/s	Particle Velocity in Explosive m/s	Shock Pressure GPa	Single Parameter Energy MJ/m ²	Dual Parameter Energy MJ/m ²	Pop Run Distance mm
700	3792	588	3.65	1.44	0.97	20.55
800	3876	668	4.35	1.95	1.43	16.31
900	3958	748	5.07	2.54	1.97	13.33
1000	4042	827	5.82	3.23	2.58	11.12
1100	4126	905	6.61	4.01	3.27	9.41
1200	4208	982	7.43	4.89	4.03	8.06

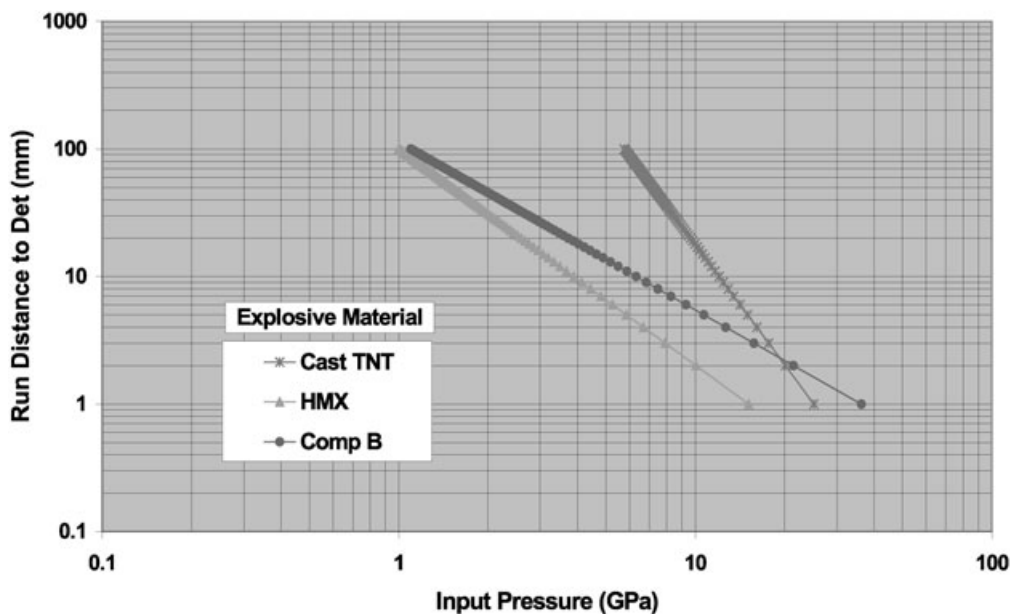


Figure 1. Pop plots for a selection of explosives

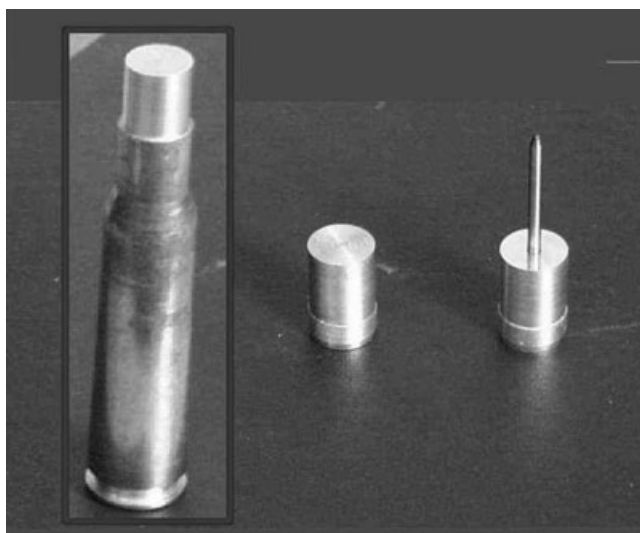


Figure 2. Flat front and shock point projectiles

4 Projectile Design Methodology

The 0.50 BMG has become an established caliber for EOD work, allowing a fairly portable selection of weapons. It has a realistic diameter, reasonable velocity range and is low cost in comparison with cannon ammunition. For this research the flat front (FF) projectile design shown in Figure 2 was chosen using a maximum bore riding diameter of 12.55 mm. Remote development work was carried out using a No 4 proof housing with an M2 heavy machine gun barrel.

4.1 Internal Ballistics

Alterations to the bullet velocity were made by varying the propellant charge and the projectile mass according to an energy conservation equation. Charge mass has been used to control a velocity range from 850 m/s to 1400 m/s, using a maximum possible compressed charge of 17.1 g (112% the standard). To attain high velocity a light 24 g (55% the standard) brass projectile has been chosen. Correspondingly, a fast burning rate propellant was chosen according to the burning rate, velocity, pressure relationship. The calculated ballistic size required for this propellant was 0.38 mm (73% the standard), and Alliant Powders Reloader 15 has been selected for these tests.

4.2 External Ballistics

High drag coefficient must be tolerated as a consequence of the flat front requirement, and calculations based on test firings estimate a peak coefficient of 1.73 at mach 2.7. To mitigate this disadvantage, the shock point (SP) design shown in Figure 2 has been developed, which at a design velocity of mach 3.8 creates an enveloping shock wave [13] according to Eq. (7). Experimental results shown in Figure 3, demonstrate that the drag coefficient for this projectile peaks before mach 2.2, declining to around 40% the value for the un-modified design at mach 2.7.

$$\sin \theta = a \cdot t / (M \cdot a \cdot t) = 1/M \quad (7)$$

For simple projectile designs, stability can be based on the gyroscopic criterion shown in Eq. (8). According to this measure, a projectile will be stable when the gyroscopic stability factor is greater than unity.

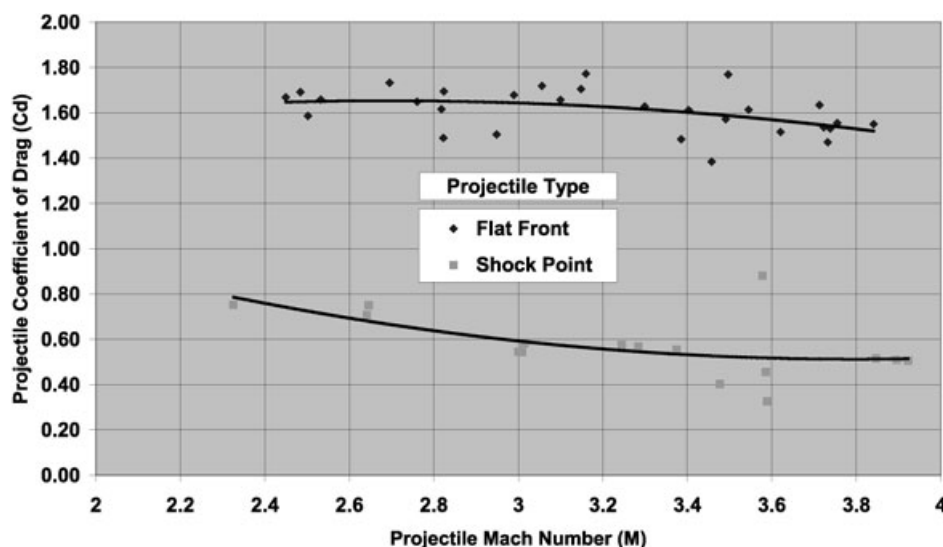


Figure 3. Drag coefficients for FF and SP projectiles

$$S_g = \frac{I_x^2 2\bar{\omega}^2}{I_y V_w^2 \rho d^3 C_{M\alpha} \pi} \quad (8)$$

Because shortening the projectile must reduce its transverse moment of inertia, this inevitably improves gyroscopic stability. These lighter projectiles are correspondingly short, and exhibit a stability factor of around 3.5 (twice the standard round).

5 Target Design Methodology

Key target characteristics were ascertained with reference to Janes Mine and Mine Clearance Handbook [14], showing that Composition-B was a prevalent explosive filling. The trend towards a lighter explosive loading was noted, with many devices employing an explosively formed projectile (EFP) kill mechanism. Casing materials of steel and plastic were common, with aluminum used in more recent NATO designs. Based on this information a pseudo-mine target has been designed to represent each of these required characteristics. The explosive fill was 1.2 kg of melt-cast Composition-B with a density of between 1680 and 1700 kg/m³. For versatility the design fits alternative barrier materials, either 1 mm of steel, 3 mm of aluminum or 5 mm of high-density polyethylene. This study has principally been concerned with high-order prompt shock events, therefore representative containment of the explosive has been a secondary issue. Figure 4 shows a pseudo-mine fitted with the mild steel barrier and instrumented ready for firing.

6 Live Firing Trials

Range instrumentation comprised three main systems. Two Kistler 211BE10 shock probes were positioned at 5 m and 10 m distance, triggered using an ionisation probe taped



Figure 4. Pseudo-mine with instrumentation

to the pseudo-mine. Make screens positioned one meter apart were used to measure projectile velocity, the second screen and I-probe can be seen taped to the mine in Figure 4. Finally, all test work has been recorded using a NAC HSV-400 video system running at 200 frames per second. Reactive events have been classified into four perceptible groups. Low-order events will be termed either 'disruptive' when no shock pressure registers, or as a 'partial reaction' when shock registers above 0.5 kPa (in both of these cases a large proportion of the explosive remains unburned). A large fireball with a pressure reading indicates 'deflagration', and a 'detonation' is recorded with an order of magnitude jump in shock pressure. The following data have been taken from a variety of barrier type and projectile velocity combinations.

Table 3. Firing results against pseudo-mine targets.

Barrier Material	Deflagration Flat Front m/s	Detonation Flat Front m/s	Detonation Shock Point m/s	Shock Point Diff %
Bare Explosive	980	969	1358	+40.1
1 mm Mild Steel	1024	1086	1044	-3.9
3 mm Aluminum	1085	1203	1207	+0.3
5 mm HDPE	1316	1348	1373	+1.9

6.1 Flat Front Projectiles. Velocity Threshold

Initially, live firings were carried out against bare explosive targets to determine a base line for prompt shock initiation. Here, the lowest projectile velocity for detonation was recorded at 969 m/s, showing considerable crossover with the deflagrative reactions. These results matched reasonably against the critical energy theory, which indicated a prompt shock threshold of 783 m/s and 896 m/s for the single and dual parameter models respectively. From this comparison, it will be observed that dual parameter critical energy theory has underestimated the velocity by just 7.5%.

Attacks were then made through three barrier materials to simulate cased mines, and the lowest velocity deflagration and detonation results have been summarized in Table 3. In each case the barrier materials have attenuated shock levels entering the explosive, producing a corresponding increase in projectile threshold velocity.

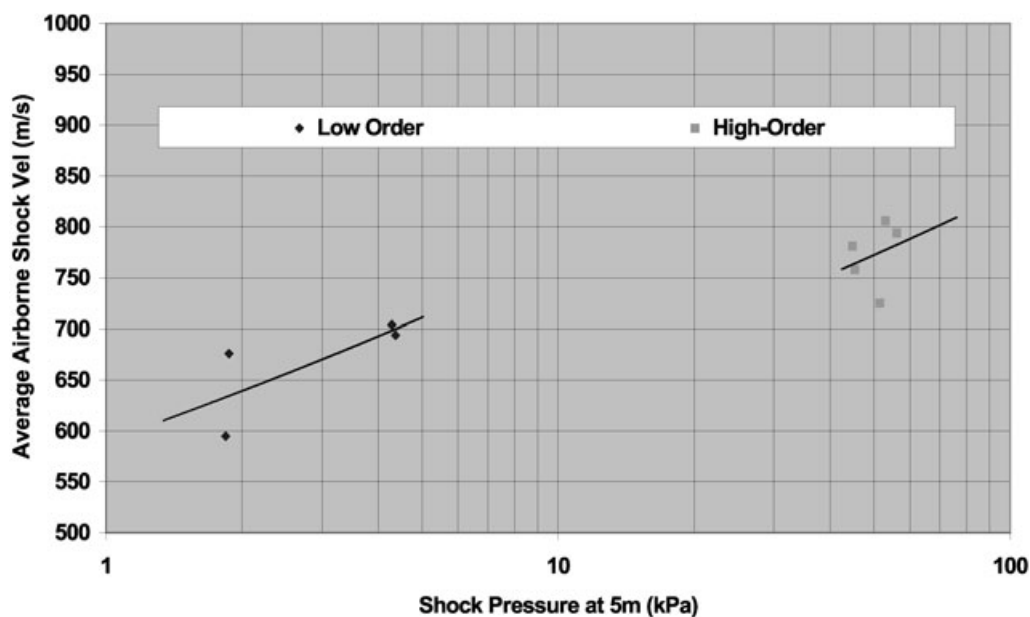
6.2 Shock Point Projectiles. Velocity Threshold

Splash range tests have shown that the shock point design has been successful in reducing drag coefficient. In addition, it was also important to assess any detrimental effect the

shock probe may have on the otherwise advantageous shock pattern afforded by a flat front design. Results from the shock point firings are also presented in Table 3, where figures for the lowest detonation velocity have been summarized in relation to flat front data. With the exception of bare explosive targets, these results show a virtually identical terminal performance. To provide a better picture of reaction order with increasing projectile velocity, shock pressure and airborne shock velocity figures have been plotted on a log scale in Figure 5. Here, the distinct jump in shock pressure between low and high order events is obvious. There is also some indication of a climbing trend in the low order zone, while the high order data tends to cluster.

7 Discussion and Conclusion

A practical limit on projectile velocity must be realised if this attack method is to be deployed using in service weapons. Therefore, it must be concluded that projectile attack with a 0.50 calibre system would only be practical against thin steel cased mines, aluminum and plastic casings both requiring impracticably high velocity because of shock attenuation.

**Figure 5.** Shock pressure and velocity for low and high order events

7.1 Inert Projectile Attack

The shock point design is clearly a superior projectile, maintaining terminal performance against contained explosive while providing a three-fold reduction in drag coefficient at higher velocity. The anomalous results against bare explosive targets were of little significance to the practical application. Here reaction development was very inconsistent, and the authors propose that higher velocity was required because of unrestrained (without the containing barrier) surface break-up just prior to flat front impact. If the prompt shock approach should be continued for future work (possibly in a larger calibre), it is recommended that the shock point route should be followed.

7.2 Critical Energy Theory

The live firing trials undertaken during this work have been compared with results reported by Cook, Haskins et al. [3], where for a 1 mm barrier their lowest velocity for detonation was just 5% faster. Our application of the single parameter critical energy calculation has produced estimates that are 19% lower than experimental values. This error is comparable with results published by other authors [2, 10] using similar projectile and velocity ranges, and pertains to the predominance of divergent shock in these projectile impact scenarios.

Further analysis using the two parameter critical energy modification [11] were undertaken, where a threshold velocity of 896 m/s has been calculated against a bare target. This theory has produced a reasonable estimation, just 7.5% lower than the measured experimental value. These results indicate that the two parameter modification is making a reasonable allowance for divergence, and is of practical value to the researcher where appropriate data can be found.

7.3 Future Work

Of the alternative neutralization methods considered, it is known that an effective low order reaction can be caused with lower levels of input energy. However, reference material and experimental practice make it clear that these phenomena are extremely difficult to model, unreliable in practice and heavily dependent on charge confinement. Therefore, it is proposed that further investigation should concentrate on understanding release wave movement and the way the shock deteriorates with travel distance. For this purpose a hydro-code model of the impact scenario has been built using a Lee-Tarver [15] representation of the explosive material, and progress with this will be reported in a later paper.

8 References

- [1] H. R. James, P. J. Haskins, M. D. Cook, Effect of Case Thickness and Projectile Geometry on the Shock Initiation Threshold for a Given Explosive. *AGARD Conference Proceedings 511*, AGARD, Neuilly s. Seine, 21–23 October 1991, pp. 18/1.
- [2] M. D. Cook, P. J. Haskins, H. R. James, Projectile Impact Initiation of Explosive Charges, *9th Symposium (International) on Detonation*, Portland, OR, August 28–September 1, 1989.
- [3] M. D. Cook, P. J. Haskins, R. Briggs, C. Stennett, Fragment Impact Characterisation of Melt Cast and PBX Explosives, Shock Compression of Condensed Matter, Atlanta, June 24–29, 2001, American Physical Society Meeting, Bulletin Vol. 46, No. 4.
- [4] C. H. Johansson, P. A. Persson, *Detonics of High Explosives*, Swedish Detonic Research Foundation, Academic Press, London and New York, 1970.
- [5] J. A. Zukas, W. P. Walters, *Explosive Effects and Applications*, Springer, Berlin, Heidelberg, New York, 1997.
- [6] P. W. Cooper, *Explosives Engineering*, Wiley-VCH, Weinheim, 1997.
- [7] T. R. Gibbs, A. Popolato, *LASL Explosive Property Data*, Los Alamos Data Centre for Dynamic Material Properties, University of California Press, 1980.
- [8] B. M. Dobratz, P. C. Crawford, *LLNL Explosives Handbook*, Report UCRL-52997, Lawrence Livermore National Laboratory, Livermore CA, 1981.
- [9] F. E. Walker, R. J. Wasley, Critical Energy for Shock Initiation of Heterogeneous Explosives. *Explosivstoffe*, 1969, 17(1), 9.
- [10] H. R. James, *An Extension to the Walker and Wasley Criterion for the Initiation of Solid Explosives by Projectile Impact*, AWRE Report No 021.82, Aldermaston, 1982.
- [11] H. R. James, An Extension to the Critical Energy Criterion used to Predict Shock Initiation Thresholds, *Propellants, Explos., Pyrotech.* 1996, 21, 8.
- [12] H. R. James, Private communication regarding use of the Dual Parameter model, October 2002.
- [13] J. G. Greenwood, et al. *Text Book of Ballistics and Gunnery*, Volumes 1 and 2, A/C 71336. Her Majesty's Stationary Office, London, 1987.
- [14] *Jane's Mines and Mine Clearance 2001–2002*, on-line at <http://online.janes.com>, June, 2002.
- [15] E. L. Lee, C. M. Tarver, Phenomenological Model of Shock Initiation in Heterogeneous Explosives, *Phys. Fluids*, 1980, 23(12), 2362.

Acknowledgement

The authors wish to sincerely thank Mr. N. Goulton and Mr. B. Lowery of QinetiQ Countermine for supporting this research program.

Symbols

a	Sound speed in air
C_{Ma}	Overturning moment coefficient derivative
C_0	Bulk sound speed, a material constant
c_x	Release wave velocity in the explosive
D	Projectile diameter
E_C	Critical energy (Walker and Wasley)
I_x	Projectile axial moment of inertia
I_y	Projectile transverse moment of inertia
M	Mach number
n	Projectile geometry number (6 for a rod)
P	Shock pressure

S_g	Gyroscopic stability factor
s	Dimensionless material constant
t	Travel time
t_D	Shock duration based on wave reflection
U	Shock velocity
U_D	Detonation shock velocity
u_p	Particle velocity in the projectile
u_x	Particle velocity in the explosive
V_w	Projectile velocity
w_e	Shock velocity in the explosive
w_p	Shock velocity in the flyer plate (Walker)
X_0	Subscript '0', pre-shock parameter

X_1	Subscript '1', post-shock parameter
x^*	Distance to detonation
Σc	Activation energy constant
Σ	Specific energy ($u^2/2$ for 1D shocks)
ρ	Density of material
ρ_a	Air density
θ	Half the included mach cone angle
ω	Projectile angular velocity

(Received July 30, 2004; revised version January 13, 2005;
Ms 2004/026)



Saved Search Alerts – Quick and Easy

Simply register. Registration is fast and free to all internet users.

Saved Search Alerts:

You are notified by e-mail whenever content is published online that matches one of your saved searches—complete with direct links to the new material.

To set a Saved Search alert: Run a search on Wiley InterScience, then click

- [Save Search](#) on the results page



Once you have saved the query, login to "My Profile" and go to **SAVED SEARCHES**. Click **+ Activate Alert** to start getting e-mail results for that query.